Article Identifier
DOI: 10.22032/dbt.58847
URN: urn:nbn:de:gbv:ilm1-2023isc-013:7

60th ILMENAU SCIENTIFIC COLLOQUIUM
Technische Universität Ilmenau, 4 – 8 September 2023
URN: urn:nbn:de:gbv:ilm1-2023isc:1

Scaling of a compliant mechanism for high-precision force measurement applications

Matthias Wolf, Martin Wittke, Mario André Torres Melgarejo, René Theska

Technische Universität Ilmenau, Institute of Design and Precision Engineering, Precision Engineering Group

ABSTRACT

This paper is dedicated to the mechanical structure of a force transducer for the measurement of very small forces in the nanonewton range with highest resolution and lowest measurement uncertainty. To achieve this, a low stiffness in one direction of motion, but high stiffness in all other directions of motion is required. Existing solutions that meet the requirements are not suitable because of their overall dimensions. This results in a need for miniaturization. For this purpose, the scaling behavior of an existing monolithic compliant mechanism is investigated and it is verified which joint contour provides an optimal stiffness ratio. It is shown that the corner-filleted contour in general has lower bending stiffnesses, but also lower cross stiffnesses compared to the semi-circular contour. A nonlinear scaling effect for the ratio of bending stiffness and cross stiffness in corner-filleted contour offers optimization potential. Based on a simplified rigid body model, additionally, the miniaturization of the mechanism is optimized. The stiffness in the desired direction of motion is reduced by about 85% compared to a semi-circular contour. The result is promising for the further development of a miniaturized force transducer. The findings of this work contribute to the advancement of the measurement of low forces and offer new perspectives for future research in miniaturized force sensors.

Index Terms – geometric scaling, compliant mechanism, stiffness, precision, force measurement

1. INTRODUCTION

This paper addresses the development of a high-resolution force transducer for the calibration of AFM cantilevers. Atomic force microscopy is widely used in nanotechnology to determine surface topologies, surface properties, and to apply forces for nanofabrication. The cantilevers used can be described by the model of a unilaterally clamped bending beam with a rectangular cross-section. Due to the cross-section, low bending stiffness is achieved in one direction, but high stiffness in all other directions of movement. From the knowledge of the stiffness behavior and the measurement of the deformation of the cantilever, the force acting on the contacted surface can be derived. The cantilevers are manufactured in high quality in a lithography process. However, residual manufacturing inaccuracies and inhomogeneities of the material lead to individual deviations of the theoretical and the real stiffness, which results in uncertainties of the force measurement and makes a calibration of the cantilevers inevitable. Three calibration methods are presented in [1], with static experimental calibration having the lowest uncertainties.

Due to the required minimum value in the nN range, the force transducer needs to have a very low stiffness in the direction of the calibration force, but a high cross stiffness in the other

directions of movement in order to be insensitive to off-center loads. The current state of the art in weighing technology provides such structures, used for high-resolution measurement of weight forces. However, due to deviating requirements, it must be verified whether such a force transducer is suitable for the position-independent calibration of cantilevers. Unlike for weight force determination, where the mechanism is precisely oriented to the vector of gravity, parasitic deformations or stiffness changes due to a change in the position of the sensor must be avoided. To allow in-situ calibration of the cantilever, the force transducer must be reduced in size from approximately 230x130x10 mm to approximately 30x30x20 mm. Therefore, this study is about the scaling behavior of the mechanism, in particular the selection of a hinge contour suitable for miniaturization.

2. STATE OF THE ART

According to [2], force measurement technology is divided into eight essential principles. They are based on the evaluation of different property changes which result from the force effect - a deformation or an acceleration. In [2], the force measurement principles are compared by comparing the force measurement range and the achievable relative measurement uncertainty. It is shown that sub-Newton ranges with low relative uncertainties can be achieved by principles with electromagnetic force compensation (EMFC). In [3] this overview is extended again by force ranges down to the nN range. It is shown that force sensors based on EMFC can serve to measure ranges from µN newton to kN. The lowest force ranges from 1 nN to a few mN are achieved by principles with electrostatic force compensation (ESFC). In [1] a force sensor based on the EMFC for the calibration of cantilevers is shown. In contrast to the mechanism of the load cells, it is characterized by a single joint and achieves a relative measurement reliability of 1.5 % at a maximum measuring force <100 nN.

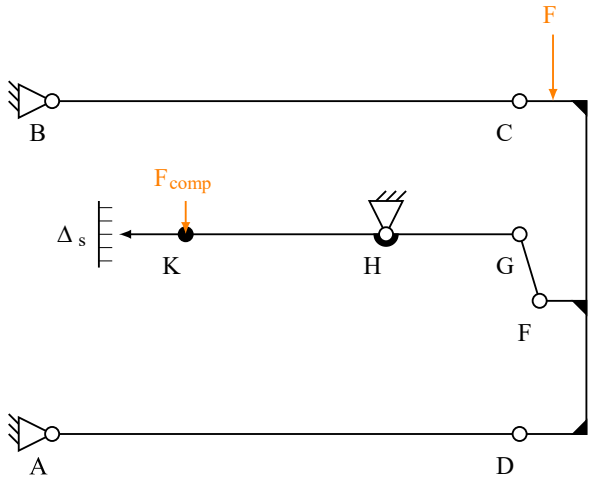

Figure 1: The principle design of the force transducer is based on a compliant mechanism. The measured force is applied at the linkage between C and D. Point K serves as the compensation point where the compensation force was applied and controlled using a position sensor.

The force measurement principle shown in Figure 1 is based on the deformation of a compliant mechanism as a result of the applied force. The deformation is measured using a high-resolution position sensor and is controlled by an actuator. Knowing the actuator constant and measuring the actuator current, a force measurement traceable to Plank's quantum of action is made possible. The lower limit of measurement range is limited by factors such as the stiffness of the compliant mechanism and the resolution of the position sensor. To achieve small initial range values, both low stiffness of the mechanism and a high-resolution position sensor are required.

State-of-the-art solutions show suitable principles for calibrating the cantilevers, but do not yet serve the required installation space, from which a direct need for research can be derived.

3. METHODS FOR THE INVESTIGATION OF THE SCALING BEHAVIOR

The existing mechanism features concentrated compliances in the form of semi-circular contour as shown in Figure 2. The aim is to investigate whether the semi-circular contour is suitable for the required miniaturization and the resulting stiffness behavior, or whether other known contours, such as the corner fillet contour, can lead to better properties. Since equally stringent requirements are placed on the force sensor in terms of positional insensitivity to gravity, the behavior of the transverse stiffnesses is also examined. The aim is a miniaturized joint with minimum bending stiffness and maximum cross stiffness in all other directions of motion.

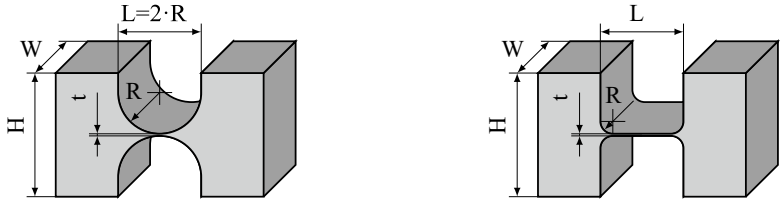

Figure 2: Representation of the joint types to be investigated; left: semi-circular contour, right: corner-filleted contour.

In [4,5,6], the scaling behavior of solid-state joints with different joint contours was considered. The scaling affected all geometry parameters of the joint and shows that the bending stiffness behaves linearly with the scaling factor S. In addition to stiffness, strain and rotational axis displacement were considered. An evaluation of the cross stiffness was not performed here. However, since the thickness t of the individual joints of the existing mechanism are already at the manufacturing limit, the thickness must be kept constant in this investigation. It is known from [6,7, 8] that the solid-state joints have minimum stiffness $K_{M_z\text{-}\theta_z}$ when the thickness is minimum. The thickness t is assumed to be t=50 µm for the study according to [9]. As [5] shows the hinge width is scaled proportional with S, so for the investigation, the hinge width is set constant to 10 mm. For the parameter study, different joint radii are investigated, each with different lengths. With the aim of achieving miniaturization of the joints, the joint length is multiplied by a scaling factor $S = 0.1\ldots1$ starting from the maximum joint length $L_{max} = 2\,R$.

4. INVESTIGATING OF SUITABLE JOINT CONTOURS

The stiffness of the joint is divided into individual components and can be described using the stiffness matrix as studied in [10, 11]:

$$\begin{bmatrix} F_x \\ F_y \\ F_z \\ M_x \\ M_y \\ M_z \end{bmatrix} = \begin{bmatrix} K_{F_x-u_x} & 0 & 0 & 0 & 0 & 0 \\ 0 & K_{F_y-u_y} & 0 & 0 & 0 & K_{F_y-\theta_z} \\ 0 & 0 & K_{F_z-u_z} & 0 & K_{F_z-\theta_y} & 0 \\ 0 & 0 & 0 & K_{M_x-\theta_x} & 0 & 0 \\ 0 & 0 & K_{F_z-\theta_y} & 0 & K_{M_y-\theta_y} & 0 \\ 0 & K_{F_y-\theta_z} & 0 & 0 & 0 & K_{M_z-\theta_z} \end{bmatrix} \begin{bmatrix} \delta_x \\ \delta_y \\ \delta_z \\ \theta_x \\ \theta_y \\ \theta_z \end{bmatrix}$$

Figure 3: Stiffness matrix according to [10,11]

The critical stiffnesses for the application are the functionally important low stiffness $K_{M_z\text{-}\theta_z}$

since this results in the lower limit of measurement range and the resolution of the force sensor according to the formula $\Delta F = \Delta s \cdot K$. Furthermore, the cross stiffness $K_{F_y\text{-}u_y}$ is of particular importance since parasitic deformations occur due to the mass of the mechanism when the position of gravity is changed.

The calculation of the individual stiffnesses is carried out via a FEM simulation with the Ansys MAPDL program. For this purpose, material-specific properties for a 7075 aluminum alloy are first parameterized using the data sheet from [12] with Young's modulus E=71 MPa and the transverse contraction number ν=0.33 for the Solid186 elements. The boundary conditions for the left side of the joint are a fixed restraint. For the bending Stiffness $K_{M_z\text{-}\theta_z}$ on the right side, an external rotational displacement around the z-axis is applied and the reaction moment was calculated to evaluate the stiffnesses. The cross stiffness was calculated using an external displacement in the y-direction by fixing the rotation around the z-axis to zero. The simulation yields the stiffness of the joint in the direction of the introduced displacement/rotation as a quotient between the occurring force/ torque reaction and the introduced displacement/ rotation.

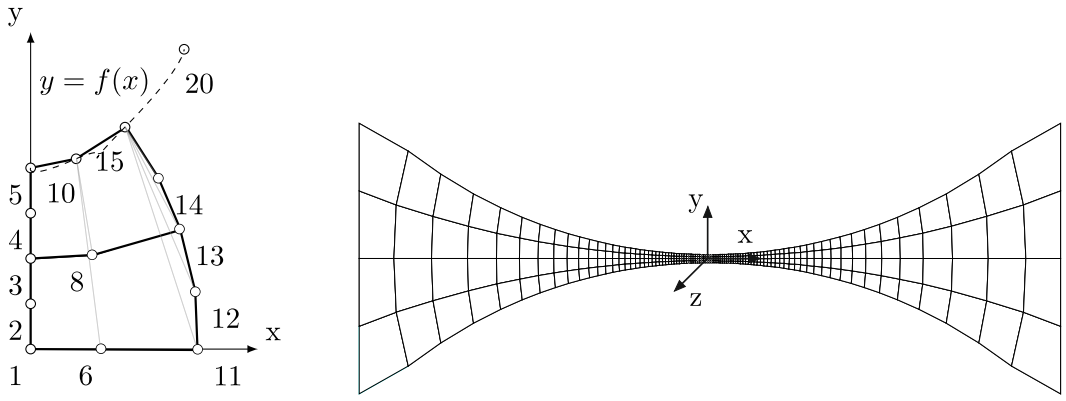

Figure 4: The FEM Modell was implemented according to the algorithm at the left site. In the right site a semi-circular hinge is presented with R/L =0.5.

The convergence of the results with the theoretical solution as a function of meshing was studied in [7, 8]. For this purpose, a significant region was defined by implementing a mesh refinement. The investigation showed that the convergence depends on the stiffnesses to be determined. For example, the significant region to achieve convergence of the stiffness $K_{F_y\text{-}u_y}$ must be 6 times the significant region for the stiffness $K_{M_z\text{-}\theta_z}$. To control these mesh properties, the joint is first created in a 2D plane. The contour of the joint is mapped using the formula for the semi-circular contour known from [5]. To create small elements in the significant thin-walled region, the y-value is divided by the number of desired elements into equally spaced elements, and one node is created at a time. The next x-value is obtained based on the spacing of the y-values as shown in Figure 4. In order to reduce the simulation time, element enlargement is allowed in the low-stress boundary regions. To implement element enlargement, the slope of the y-values is included in the calculation of the x-value to be generated, with the effect of the slope weakening from the contour of the joint to the neutral fiber. Plane183 elements are then generated based on the created nodes. The advantage of the generation of the individual nodes is that the meshing can be generated and parameterized completely independently. Finally, a 3D model of Solid186 elements is extruded from the 2D Plane183 elements. The parameter study is performed by calling the MAPDL script in Ansys Workbench. Thus, the desired parameters for radius and length can be inserted and calculated automatically.

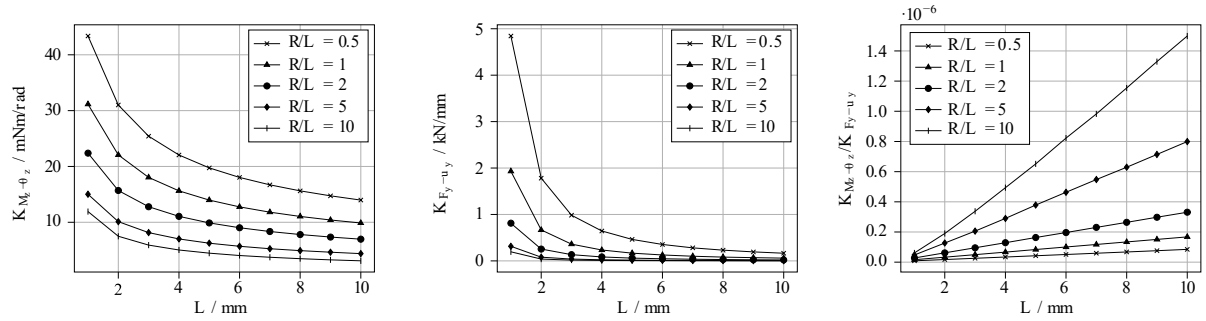

(a) semi circular hinge - bending stiffness $K_{M_z-\theta_z}$

(b) semi circular hinge - cross stiffness $K_{F_y-u_y}$

(c) semi circular hinge - relationsship between bending and cross stiffness $\frac{K_{M_z-\theta_z}}{K_{F_y-u_y}}$

Figure 5: Comparison of the stiffnesses of a semi-circular hinge

In the diagrams in Figure 5 the relationship between the stiffnesses to radius *R* and joint length *L* is shown. The radius is parametrized as the relationship between radius and length, where the ratio *R*/*L*=0.5 means fully designed hinge contours and larger ratios lead to cutting off the hinge contours by means of its length. After evaluating all stiffnesses, only the stiffnesses critical to the application are presented in this paper. Besides the stiffness $K_{M_z-\theta_z}$, which is important for the function, the stiffness $K_{F_y-u_y}$ is most relevant. It is shown that the desired minimum stiffness $K_{M_z-\theta_z}$. is achieved at large radii and large joint lengths, with the stiffness converging to a minimum at a scaling factor of *S*=0.2. A similar behavior can be observed for the transverse stiffness $K_{F_y-u_y}$ in diagram (b) in Figure 5. The cross stiffness approaches a minimum converging at a scaling factor of approximately *S*=0.6. With larger radii *R*, the cross stiffness $K_{F_y-u_y}$ decreases. The ratio between the stiffness $K_{M_z-\theta_z}$. and the cross stiffness $K_{F_y-u_y}$ is shown in the diagram (c) in Figure 5. The aim is to achieve small ratios with the smallest possible scaling factors. In this respect, joints with small joint lengths *L* and small radii *R* are preferable.

Since the reduction of the bending stiffness $K_{M_z-\theta_z}$. is functionally important, an investigation is currently being carried out with regard to the corner filleted joint as shown in Figure 2. According to the previous investigation, joints with large radii and short lengths achieve the lowest bending stiffness. In practice, this type of joint can be found as leaf spring joints. The expected optimization motivates further investigation. Since the mechanism should exploit all the advantages of monolithically manufactured joints, a corner filleted contour is investigated instead of the leaf-spring contour. Similar to the semi-circular joint, the influence of different radii with different lengths is investigated. The minimum radius depends on the manufacturing process and is about 0.3 mm when using a wire electro-discharging machine (WEDM) [13]. The minimum length to be investigated is twice the radius and is scaled with a scaling factor S=1...10. The MAPDL script is created analogous to the semi-circular joint with the formula for the contour known from [5]. The radius-length ratios of *R*/*L*=0.05…0.5 are examined, where *R*/*L*=0.05 is a corner-filleted hinge with small radii and large length and *R*/*L*=0.5 corresponds to a semi-circular joint.

The results of the simulations are shown in the diagrams (a)-(b) in Figure 6. Small bending stiffnesses $K_{M_z-\theta_z}$. are obtained as expected for large joint lengths and small radii. The comparison with the semi-circular joint shown as *R*/*L*=0.5 indicates that significantly lower bending stiffnesses $K_{M_z-\theta_z}$. can be achieved. However, the cross stiffness $K_{F_y-u_y}$ of the

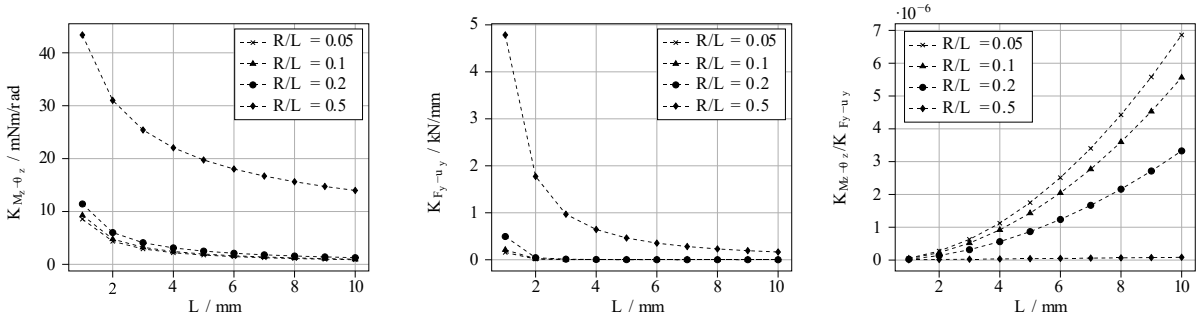

(a) corner-filleted hinge - bending stiffness $K_{M_z-\theta_z}$

(b) corner-filleted hinge - cross stiffness $K_{F_y-u_y}$

(c) corner-filleted hinge - relationsship between bending and cross stiffness $\frac{K_{M_z-\theta_z}}{K_{F_y-u_y}}$

Figure 6: Comparison of the stiffnesses of a corner-filleted hinge

investigated corner-filleted joint contours behave in an analogous manner. Large cross stiffnesses $K_{F_y\text{-}u_y}$ are obtained as expected with large radius and small joint length, as is the case with the semi-circular contour. The ratio of bending stiffness $K_{M_z\text{-}\theta_z}$. to cross stiffness $K_{F_y\text{-}u_y}$ shown in diagram (c) Figure 6 indicates that the desired low ratios are achieved with short joint lengths and large radii.

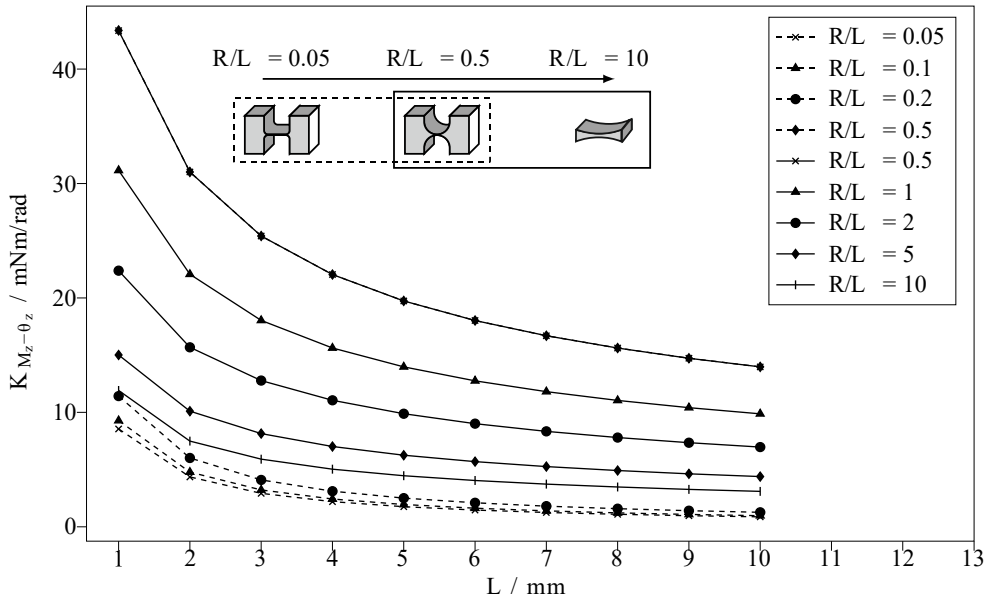

Figure 7: Comparison the bending stiffness of a semi-circular hinge and a corner- filleted hinge

To compare the ratio between semi-circular and quarter-circular contours, the bending stiffness $K_{M_z\text{-}\theta_z}$, as well as the bending/ cross stiffness ratio $K_{M_z\text{-}\theta_z}/K_{F_y\text{-}u_y}$ are compared in the diagrams in Figures 7 and 8. As it is shown the lowest bending stiffness $K_{M_z\text{-}\theta_z}$ is achieved with the corner-filleted hinge contour. The comparison of the bending/ cross stiffness ratio $K_{M_z\text{-}\theta_z}/K_{F_y\text{-}u_y}$ shows that better ratios are achieved for large joint lengths with semi-circular contours. For small joint lengths, however, good ratios are also achieved by the corner-filleted joints, which is due to the nonlinear behavior.

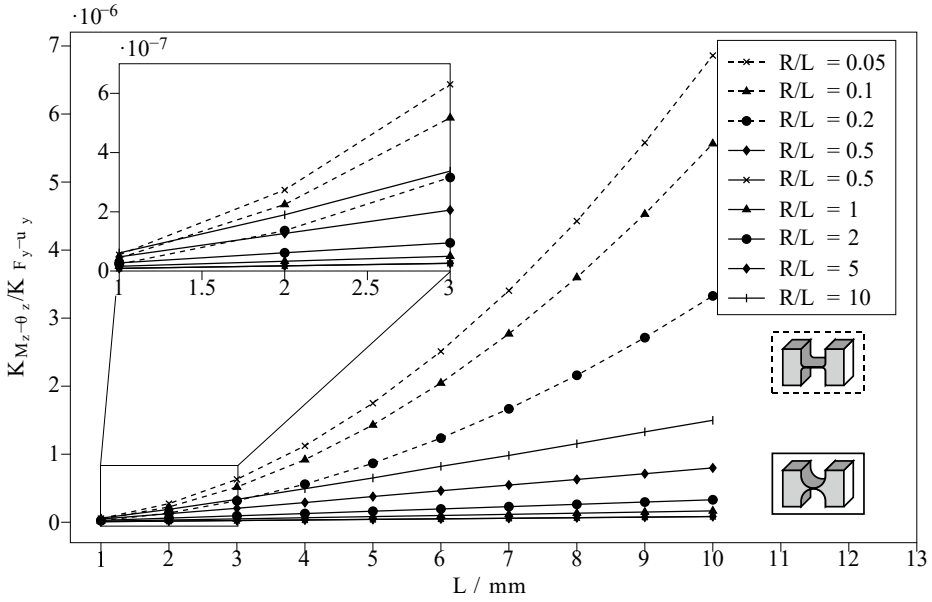

Figure 8: Comparison the cross stiffness of a semi-circular hinge and a corner- filleted hinge

Therefore, a corner-filleted contour with R=0.3 mm and a joint length L= 2 mm is chosen for the following investigation. This results in a bending stiffness of $K_{M_z\text{-}\theta_z}$= 5.320 mNm/rad and a cross stiffness of $K_{F_y\text{-}u_y}$= 26314.115 N/m. For comparison even a semi-circular contour with $R = 10\,mm$ and a joint length $L = 2\,mm$ was investigated. Its stiffness parameters are $K_{M_z\text{-}\theta_z}$= 10.635 mNm/rad and $K_{F_y\text{-}u_y}$= 80678.217 N/m.

5. RIGID BODY MODELL

To investigate the structural stiffness of the mechanism in the working direction, a highly simplified rigid body model is first used. The joints (A-H) are modeled with the previously

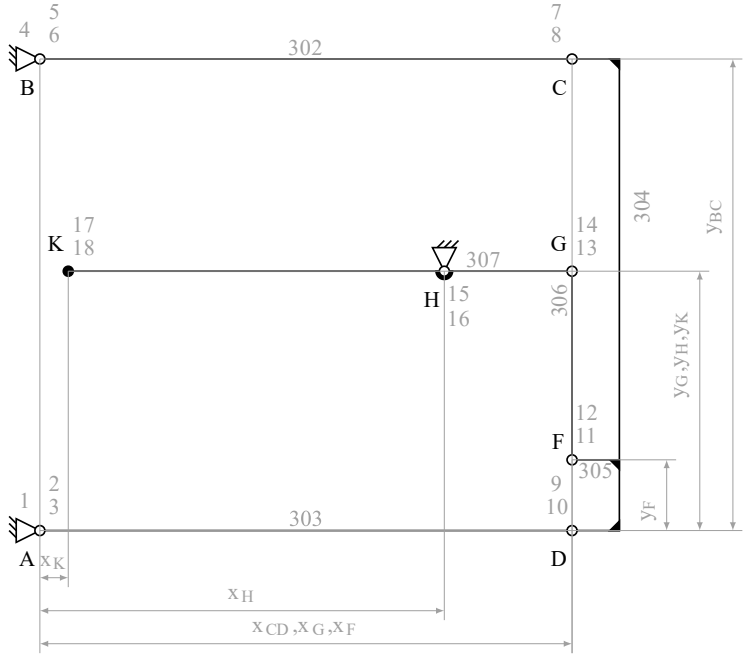

Figure 9: Rigid-body model of the weighing mechanism

determined stiffness matrix. The joints are connected to each other by rigid beam elements, the deformation of which, due to the small forces introduced, is not considered in this preliminary investigation. The mechanism is rigidly connected to the frame at joints A, B and H. The point K is the working point of the mechanism. Point K is the working point of the mechanism at which force compensation and position measurement are performed in the real model. The force to be measured is introduced at point C. In the rigid-body model, point K is used to introduce an external displacement. In the simulation software the external displacement is used to calculate the resulting reaction force at point K and determines the stiffness K of the mechanism in the working direction via the ratio of the reaction force to the external displacement.

Table 1: Geometry parameter for the rigid-body model

Geometry parameter	Value
x_{CDFG}	112.5 mm
x_{K}	6 mm
x_{H}	85.5 mm
y_{BC}	100 mm
y_{GHK}	55 mm
y_{F}	15 mm

The model is implemented using the input parameters for geometry generation, joint stiffness and the specification of the introduced displacement at point K. The geometry parameters are taken from the design of the existing load cell and are shown in Table 1. The joint bending stiffnesses $K_{M_z\text{-}\theta_z}$ is used from the previous investigation. The corner filleted joints are subject of the main investigation. For comparison, the semi-circular contours are still shown.

The system stiffness K_{syst} in the working direction is the output of the program. The rigid body model was implemented based on the simulation software Mechanical APDL Ansys. As an interface between the simulation software and the input and output parameters, the Python programming environment was chosen and implemented using object-oriented programming.

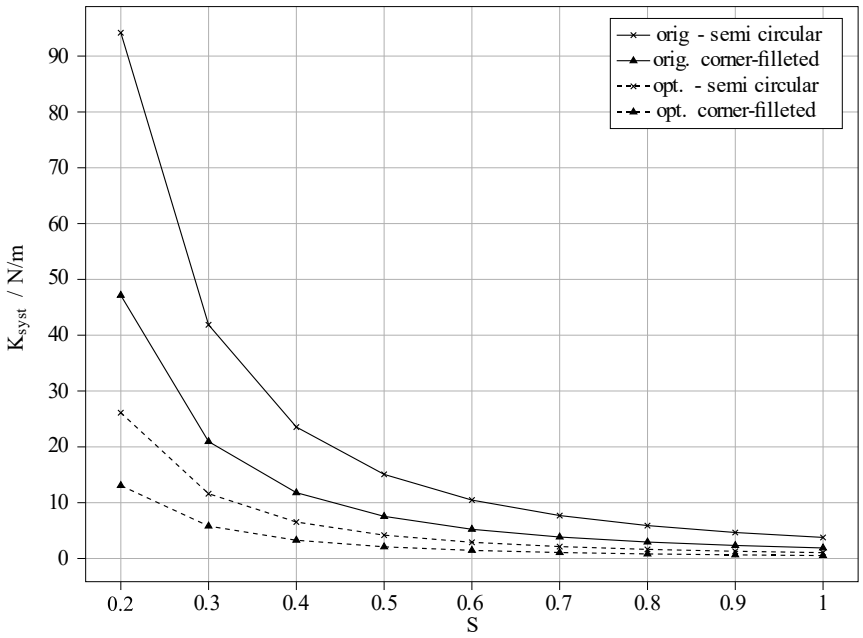

Figure 10: Representation of the scaling behavior with semi-circular hinge and corner-filleted hinge contour with original and optimized geometry parameters

This offers the possibility to vary the rigid body model with different geometry parameters to calculate the system stiffness.

The dependence of the structural stiffness on the scaling of the mechanism is investigated. For this purpose, the geometry parameters from table 1 are multiplied by the scaling factor S. The joints and thus the bending stiffness $K_{M_z\text{-}\theta_z}$ remain independent of the scaling factor, which is justified by the limit of the manufacturing parameters as well as the manufacturability. With the geometry parameters in the table 1, the behavior for the system stiffness K_{syst} is shown in Figure 10. The system stiffness K_{syst} scales with the miniaturization of the system with $\frac{1}{s^2}$.

Of further interest is the investigation of the structural stiffness behavior depending on the variation of individual geometry parameters. The investigation is conducted using the existing rigid body model. The geometry parameters are evaluated successively in the simulation program and the influence on the system stiffness. In summary, the parameters with their correlation with respect to a stiffness minimization are presented in Table 2. Based on the obtained knowledge, the structure is reparametrized and the results were presented in Table 2 and Figure 10 as the dashed lines.

Table 2: Geometry parameter and the resulting stiffnesses with corner-filleted contour

Geometry parameter	Behavior	Original value	Optimized value
x_{CD}	negligible	112.5 mm	112.5 mm
x_F	negligible	112.5 mm	116 mm
x_G	minimize	112.5 mm	115 mm
x_K	minimize	6 mm	-20 mm
x_H	maximize	85.5 mm	105 mm
y_{BC}	negligible	100 mm	100 mm
y_G	maximize	55 mm	81 mm
y_H	minimize	55 mm	53 mm
y_K	negligible	55 mm	53 mm
y_F	negligible	15 mm	25 mm
System stiffness with scaling factor S = 1		1.885 N/m	0.522 N/m
System stiffness with scaling factor S = 0.2		47.14 N/m	13.069 N/m

6. CONCLUSION

This paper presents the investigation on miniaturization of a force transducer consisting on a monolithically fabricated compliant structure. First, the individual joints with semi-circular and corner-filleted contours were compared in terms of miniaturization behavior. The trend shows that the corner-filleted joints are particularly suitable for small joint lengths. After the investigation of the individual joints, the force transducer was abstracted in a rigid body model and implemented with the determined joint stiffnesses. It can be shown that a stiffness minimization of approx. 70% can be achieved with the use of corner-filleted joints. By optimizing the geometry, the stiffness could be reduced again by about 70%.

Furthermore, the influence with regard to the orientation to gravity should be investigated. This will be simulated on a 3D FEA model and then verified experimentally on a manufactured prototype.

Acknowledgement

The authors would like to thank the German Research Foundation (DFG) for the financial support of the project.

REFERENCES

[1] O. Dannberg, T. Fröhlich, "Steifigkeitsmessungen von AFM-Cantilevern", tm - Technisches Messen 88, DE GRUYTER, Oldenbourg, 88(S1): S3 -S7, 2021.
[2] R. Schwartz, "Kraft, Masse, Drehmoment." In: Gevatter, HJ., Grünhaupt, U. (eds) Handbuch der Mess- und Automatisierungstechnik in der Produktion. VDI-Buch. Springer, Berlin, Heidelberg, pp. 55-92, 2006.
[3] R. R. Marangoni, "Traceable Multicomponent Force and Torque Measurement" 2019.
[4] P. Gräser, S. Linß, T. Räder, L. Zentner, R. Theska, "Investigations of the geometrical scaling in the systematic synthesis of compliant mechanisms", euspen's 18th International Conference & Exhibition, Venice, IT, June 2018
[5] S. Linß, P. Gräser, T. Räder, S. Henning, R. Theska, L. Zentner, "Influence of geometric scaling on the elasto-kinematic properties of flexure hinges and compliant mechanisms", Mechanism and Machine Theory Volume 125, Elsevier Ltd., pp. 220-239, 2018
[6] T. Räder, S. Linß, P. Gräser, R. Theska, "Systematische Untersuchung der Einflüsse geometrischer Skalierung von nachgiebigen Koppelmechanismen mit optimierten Festkörpergelenken", 2017
[7] M. Torres, M. Darnieder, S. Linß, R. Theska, J.R.Hernández, "Modeling of the elastic mechanical behavior of thin compliant joints under load for highest-precision applications", 2018
[8] N. Xu, M. Dai, X. Zhou, "Analysis and design of symmetric notch flexure hinges", Advances in Mechanical Engineering Vol 9(11), Sage, pp. 1-12, 2017.
[9] D. Schoenen, S. Lersch, M. Hüsing, B. Corves, F. Klocke, L. H. Andreas, "Entwicklung, Konstruktion und Anwendung eines Prüfstands zur Ermittlung der ertragbaren Lastzyklen filigraner hochgenauer stoffschlüssiger Gelenke", Kolloquium Getriebetechnik, Garching, pp. 169-181, 2015.
[10] N. Lobontiu, E. Garcia, M. Hardau, N. Bal; "Stiffness characterization of corner-filleted flexure hinges.", Rev Sci Instrum 75 (11), pp. 4896–4905, 2004
[11] S. Yiping, L. Xin, W. Songlai, L. Xuejun, "Dynamic Analysis of a 5-DOF Flexure-Based Nanopositioning Stage.", Mathematical Problems in Engineering (11), Hindawi, 2019
[12] https://gleich.de/de/produkte/en-aw-7075/ (20.05.2023)
[13] V. Patel, A. Darji; "An experimental investigation of wire-EDM for aluminum 7075-T6.", GJRA – Global Journal for research, pp. 709-711, 2017

CONTACTS

M. Sc. Matthias Wolf — email: matthias.wolf@tu-ilmenau.de
ORCID: https://orcid.org/0009-0002-1446-882X

M. Sc. Martin Wittke — email: martin.wittke @tu-ilmenau.de
ORCID: https://orcid.org/0000-0002-2743-1770

M. Sc. Mario André Torres Melgarejo — email: mario.torres@tu-ilmenau.de
ORCID: https://orcid.org/0000-0003-1713-6273

Univ.- Prof. Dr.-Ing. René Theska — email: rene.theska@tu-ilmenau.de
ORCID: https://orcid.org/0000-0003-0589-8270

